Monthly Notices of the ROYAL ASTRONOMICAL SOCIETY
MNRAS **449,** 1614–1624 (2015) doi:10.1093/mnras/stv266

First EURONEAR NEA discoveries from La Palma using the INT*

O. Vaduvescu,[1,2,3]† L. Hudin,[4] V. Tudor,[1] F. Char,[5] T. Mocnik,[1] T. Kwiatkowski,[6] J. de Leon,[2,7] A. Cabrera-Lavers,[2,7] C. Alvarez,[2,7] M. Popescu,[3,8] R. Cornea,[9]‡ M. Díaz Alfaro,[1,2,7] I. Ordonez-Etxeberria,[10,1] K. Kamiński,[6] B. Stecklum,[11] L. Verdes-Montenegro,[12] A. Sota,[12] V. Casanova,[12] S. Martin Ruiz,[12] R. Duffard,[12] O. Zamora,[2,7] M. Gomez-Jimenez,[2,7] M. Micheli,[13,14,15] D. Koschny,[16] M. Busch,[17] A. Knofel,[18] E. Schwab,[19] I. Negueruela,[20] V. Dhillon,[21] D. Sahman,[21] J. Marchant,[22] R. Génova-Santos,[2,7] J. A. Rubiño-Martín,[2,7] F. C. Riddick,[1] J. Mendez,[1] F. Lopez-Martinez,[1] B. T. Gänsicke,[23] M. Hollands,[23] A. K. H. Kong,[24] R. Jin,[24] S. Hidalgo,[2,7] S. Murabito,[2,7] J. Font,[2,7] A. Bereciartua,[2,7] L. Abe,[25] P. Bendjoya,[25] J. P. Rivet,[25] D. Vernet,[26] S. Mihalea,[9] V. Inceu,[10] S. Gajdos,[27] P. Veres,[27] M. Serra-Ricart[2,7] and D. Abreu Rodriguez[28]

Affiliations are listed at the end of the paper

Accepted 2015 February 6. Received 2015 February 6; in original form 2015 January 21

ABSTRACT

Since 2006, the European Near Earth Asteroids Research (EURONEAR) project has been contributing to the research of near-Earth asteroids (NEAs) within a European network. One of the main aims is the amelioration of the orbits of NEAs, and starting in 2014 February we focus on the recovery of one-opposition NEAs using the Isaac Newton Telescope (INT) in La Palma in override mode. Part of this NEA recovery project, since 2014 June EURONEAR serendipitously started to discover and secure the first NEAs from La Palma and using the INT, thanks to the teamwork including amateurs and students who promptly reduce the data, report discoveries and secure new objects recovered with the INT and few other telescopes from the EURONEAR network. Five NEAs were discovered with the INT, including 2014 LU14, 2014 NL52 (one very fast rotator), 2014 OL339 (the fourth known Earth quasi-satellite), 2014 SG143 (a quite large NEA), and 2014 VP. Another very fast moving NEA was discovered but was unfortunately lost due to lack of follow-up time. Additionally, another 14 NEA candidates were identified based on two models, all being rapidly followed-up using the INT and another 11 telescopes within the EURONEAR network. They include one object discovered by Pan-STARRS, two Mars crossers, two Hungarias, one Jupiter trojan, and other few inner main belt asteroids (MBAs). Using the INT and Sierra Nevada 1.5 m for photometry, then the Gran Telescopio de Canarias for spectroscopy, we derived the very rapid rotation of 2014 NL52, then its albedo, magnitude, size, and its spectral class. Based on the total sky coverage in dark conditions, we evaluate the actual survey discovery rate using 2-m class telescopes. One NEA is possible to be discovered randomly within minimum 2.8 deg^2 and maximum 5.5 deg^2. These findings update our past statistics, being based on double sky coverage and taking into account the recent increase in discovery.

Key words: methods: observational – surveys – astrometry – minor planets, asteroids: general.

* Based on override time (Spanish and UK programmes C136/2014A, C88/2014B and P2/2014B) and some D-time observations made with the Isaac Newton Telescope (INT) operated on the island of La Palma by the Isaac Newton Group (ING) in the Spanish Observatorio del Roque de los Muchachos (ORM) of the Instituto de Astrofísica de Canarias (IAC).

† E-mail: ovidiu.vaduvescu@gmail.com
‡ Amateur astronomer, Romania.

1 INTRODUCTION

Near-Earth Asteroids (NEAs) are defined as minor planets with a perihelion distance (q) less than 1.3 au (Morbidelli et al. 2002; JPL 2015). Currently, the NEA population includes four major classes, namely Amors, Apollos, Atens and Atiras. Potentially hazardous asteroids (PHAs) are defined as NEAs having a minimum orbital intersection distance (MOID) less than 0.05 au and the absolute magnitudes (H) less than 22 mag, which corresponds to objects larger than about 150 m. This limit in size represents the asteroids large enough to potentially cause a global climate disaster and threaten the continuation of human civilization.

We know today (2015 Jan) more than 12 000 NEAs (MPC 2015), mostly discovered by a few dedicated surveys funded in the US using 1m class telescopes (Catalina, LINEAR, Spacewatch, NEAT, LONEOS) and more recently by Pan-STARRS 1.8 m (Jedicke et al. 2007) and the *WISE*/*NEOWISE* 0.6 m infrared space surveys (Wright et al. 2010; Mainzer et al. 2011). Some other 10 000 NEAs larger than 100 m were estimated to exist (Mainzer et al. 2012), most of them falling within 2-m class discovery capabilities (Vaduvescu et al. 2013a).

Part of the known NEA population, about 400 objects have poor orbital data, being unobserved for years and having orbits calculated based on small arcs spanning a few weeks or days following discovery, resulting in more uncertain recoveries and in some cases in marginal or bad matches and lost objects. The amelioration of such NEA orbits is an opportunity for 2-m class telescopes equipped with relatively large field imaging cameras, including the Isaac Netwon Telescope (INT) operated on the island of La Palma by the Isaac Newton Group (ING) in the Spanish Observatorio del Roque de los Muchachos (ORM) of the Instituto de Astrofísica de Canarias (IAC).

Since 2006, the European Near Earth Asteroids Research (EURONEAR) has contributed mainly to the orbital amelioration of NEAs within a European network (Vaduvescu et al. 2008) which includes now 20 European and one Chilean nodes. For this project, we used mostly 1–4 m telescopes and a few other smaller facilities available to our network (Birlan et al. 2010a,b; Vaduvescu et al. 2011a, 2013a) plus archival imaging taken by 2–4 m telescopes (Vaduvescu et al. 2009, 2011b, 2013b). During the last eight years, we have succeeded in improving about 1500 NEA orbits (Vaduvescu et al. 2014), thanks to the collaboration with about 30 students and amateur astronomers from Romania, Spain, UK, Chile, Germany and France, who have been actively involved in data reduction, observations, discoveries, data mining, software and data base development, working together mostly remotely via the internet. Beside the above papers, this work produced around 100 MPC/MPEC publications (Vaduvescu et al. 2008–2014) and more than 10 contributions in international conferences.

Since 2014 February, part of the ING Spanish and UK regular calls, EURONEAR has been granted time for three observing proposals (the Spanish C136/2014A, C88/2014B and the UK P2/2014B) to use the INT telescope endowed with the Wide Field Camera (WFC) for the programme 'Recovering NEAs and Eliminating VIs: A Pilot ToO Program with the INT-WFC' (Vaduvescu et al. 2015). By securing a few dozen short triggers (max 1h/night) throughout two semesters, our team is aiming to recover about 200 one-opposition faint (mostly $22 < V < 23$) and uncertain ($\sigma < 20$ arcmin) NEAs, and also to discover and secure promptly a few NEAs serendipitously observed in the programme fields. Although in the past years EURONEAR serendipitously discovered but could not secure a few NEAs (Vaduvescu et al. 2013a), since 2014 February, we started to secure our NEA discoveries thanks to the conjunction of three essential factors: the very fast data reduction in a team comprising about 10 amateur astronomers and students (including some ING students), the INT override opportunity and the involvement of a few EURONEAR nodes and collaborators able to access other mostly 1m class telescopes for rapid follow-up. By meeting these conditions, since 2014 June EURONEAR discovered and secured the first five NEAs ever discovered from La Palma and using the INT.

In Section 2, we introduce the INT observations and data reduction. In Section 3, we present the circumstances of our NEA discoveries, while in Sections 4 and 5 we discuss two special objects, namely the very fast rotator 2014 NL52 and the Earth quasi-satellite 2014 OL339. In Section 6, we re-assess the unknown NEA sky density accessible to 2-m surveys nowadays, and in Section 7 we discuss future strategy and work in progress.

2 OBSERVATIONS AND DATA REDUCTION

All discovery observations were acquired in La Palma using the 2.5 m INT telescope during two regular visiting nights plus three of INT D-nights. The follow-up work (consisting of a few follow-up nights for astrometry and photometry) was carried out using the 2.5 m INT telescope (all objects) and some fields were followed-up using another 11 telescopes of the EURONEAR network or other collaborators: the 1.5 m in Sierra Nevada Observatory (OSN), Tautenburg 2 m TLS in Germany, the 2 m LT, the 4.2 m William Herschel Telescope (WHT) and Mercator 1.2 m in La Palma, the 1 m ESA Optical Ground Station (ESA-OGS) and IAC80 0.8 m in Tenerife, C2PU 1 m in France, Modra 0.6 m in Slovakia, Poznan 0.7 m (PST2) in Arizona and GLORIA D50 0.5 m in Ondrejov (remotely controlled). In Table 1, we include the main characteristics of these facilities. We are indebted and we offered co-authorship to all these involved collaborators.

At the prime focus of the INT, we used the WFC which consists of four CCDs $2k \times 4k$ pixels, covering an L-shaped 34 arcmin × 34 arcmin field with a pixel scale of 0.33 arcsec pixel^{-1}. All WFC frames were observed with no binning and using slow readout (48 s). During all runs, we used the Sloan r filter to avoid fringing and minimize twilight and any possible moonlight. For all fields, we tracked all our main targets (the known one-opposition NEAs) at their half proper motion. We used in all cases sequences of six to eight times 120 s exposures, needed to detect most of our faint targets typically around $22 < V < 23$. Most of the nights were dark with good seeing (typical average 1.2 arcsec for the INT) and low airmass for all fields (better than 1.4).

For data reduction, first we used THELI (Erben et al. 2005; Schirmer 2013) to subtract the bias and twilight flat and to correct the known field distortion at the prime focus of the INT. Secondly, we used ASTROMETRICA software (Raab 2015) with a fit order 1–2 and PPMXL or UCAC4 catalogues, to detect all moving sources via human blink (typically a few dozen known or unknown main belt asteroids in each field). As the third quality control step, we used the FITSBLINK (Skvarc 2015) and the EURONEAR O−C (observed minus calculated) servers, also the Minor Planet Center (MPC) NEO rating tool and finally the FIND_ORB software (Gray 2015) to check the astrometry and confirm the target NEA based on orbital fits. Reducing all data in a team of about 10 experienced students and amateurs, we could classify, measure and report all the INT detections from all the fields to MPC, within one day.

Table 1. The main characteristics of the telescopes involved in NEA discoveries: observatory, telescope diameter (metres), camera name, pixel scale (arcsec pixel^{-1}), field of view (in arcmin), non-sidereal rate, typical instrumental seeing (arcsec) and limiting magnitude V at S/N = 5 detection in dark time one-minute exposure at Zenith.

Observatory	Telescope	Diam	Camera	FOV	Scale	Track	Seeing	Lim.mag
ORM La Palma	INT	2.5	WFC	34 × 34	0.33	yes	1.2	23.0
ORM La Palma	WHT	4.2	ACAM	8 (diam)	0.25	yes	0.8	24.0
ORM La Palma	LT	2.0	RISE	9 × 9	0.54	yes	2.0	21.5
ORM La Palma	Mercator	1.2	MAIA	9 × 14	0.28	yes	1.0	21.5
OSN Spain	T150	1.5	VersArray	8 × 8	0.20	yes	1.5	21.0
TLS Germany	Schmidt	1.3	Prime	42 × 42	1.20	yes	2.0	20.5
Calern France	C2PU	1.0	SBIG STX16803	38 × 38	0.56	yes	2.0	20.5
OT Tenerife	ESA-OGS	1.0	custom	48 × 48	0.70	yes	1.5	20.5
OT Tenerife	IAC80	0.8	CAMELOT	10 × 10	0.30	no	1.2	20.5
Winer Arizona	PST2/Poznan	0.7	iXon888	10 × 10	0.58	yes	2.0	20.0
Modra Slovakia		0.6	Apogee AP-8	25 × 25	1.47	yes	2.5	20.0
GLORIA Ondrejov	D50	0.5	FLI IMG 4710	20 × 20	1.20	no	2.0	19.0

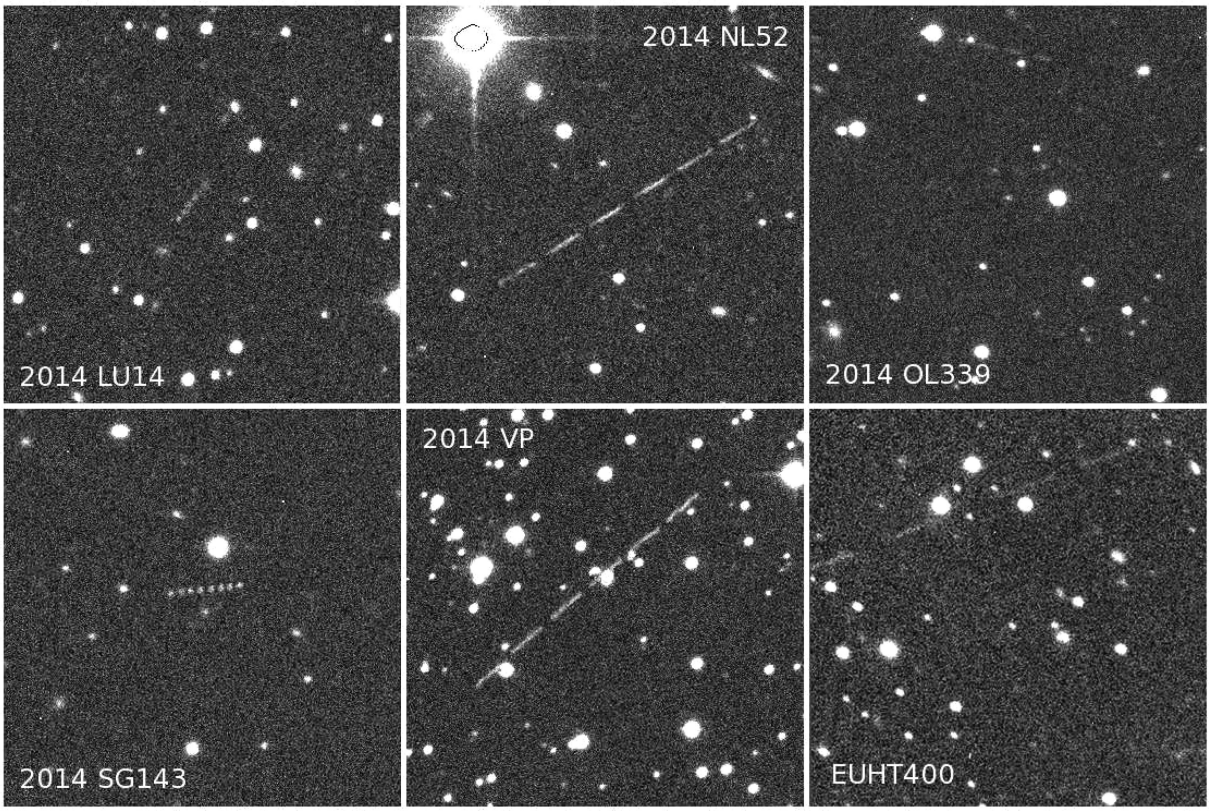

Figure 1. NEA discovery stack images. The field of view (FOV) is 2 arcmin × 2 arcmin in normal sky orientation. 2014 OL339 could be barely seen in the upper side, while for EUHT400 we include only the last four of the available six images.

3 DISCOVERED NEAS AND OTHER NEA CANDIDATES

In Fig. 1, we include the discovery images (composite of all frames) and in Table 1 we include the log and discovery circumstance data for our six discovered NEAs and other 14 follow-up NEA candidates discussed in Section 3.7. We include the observers, data reducers and actual discoverer (in bold), the official designation, EURONEAR nickname, discovery date (UT of the first image), observed field (typically known one-opposition NEAs), the apparent proper motion μ (in arcsec min^{-1}), solar elongation (in degrees), MPC NEO Int score (between 0 and 100), the exposure time (in seconds) and number of images, measured R-band magnitude, orbital elements (estimated by FIND_ORB for very short orbits) semimajor axis a (in astronomical units au), eccentricity e, inclination i (degrees), MOID (au), absolute magnitude H, orbit type, number of EURONEAR follow-up nights FN and actual orbital arc (days or minutes).

In Fig. 2, we plot the discovered objects in the ϵ–μ model (Vaduvescu et al. 2011a) which allowed us to distinguish and follow-up all NEA candidates, together with their MPC NEO rating score. In Figs 3 and 4, we plot in solid circles the orbital elements of our five discovered NEAs and with crosses the other NEA candidates,

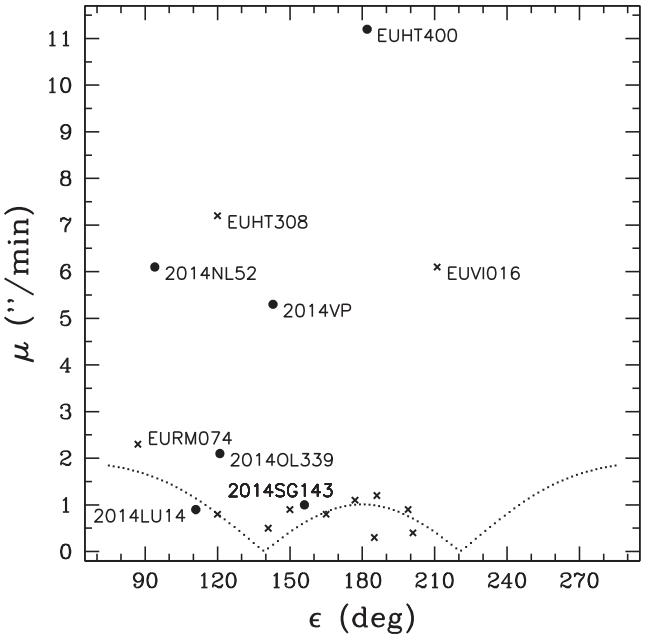

Figure 2. The ϵ–μ model (Vaduvescu et al. 2013b) plotting the apparent proper motion μ versus Solar elongation ϵ used to distinguish rapidly between MBAs and NEA candidates located above the magenta dotted line roughly defining the NEA limit. We plot in solid circles our five secured NEAs plus EUHT400, and with crosses the other 12 NEA candidates.

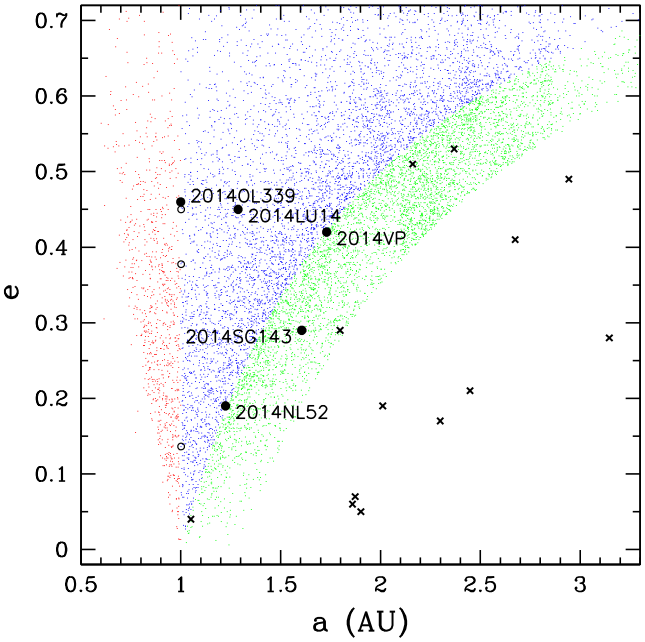

Figure 3. The classical *a*–*e* orbital distribution (eccentricity versus semimajor axis) including our discoveries (solid circles) and other NEA candidates (crosses) with respect to the entire known Amors (green dots), Apollos (blue) and Atens populations (red dots). With open circles, we plot the other three known Earth quasi-satellites, in comparison with 2014 OL339. The Jupiter trojan 2014 RC13 is located outside the plot ($a = 5.2$ au).

drawing with green, blue and red dots the entire known Amors, Apollos and Atens, respectively. We discuss briefly here the discovery circumstances and orbital parameters in the entire known NEA population context.

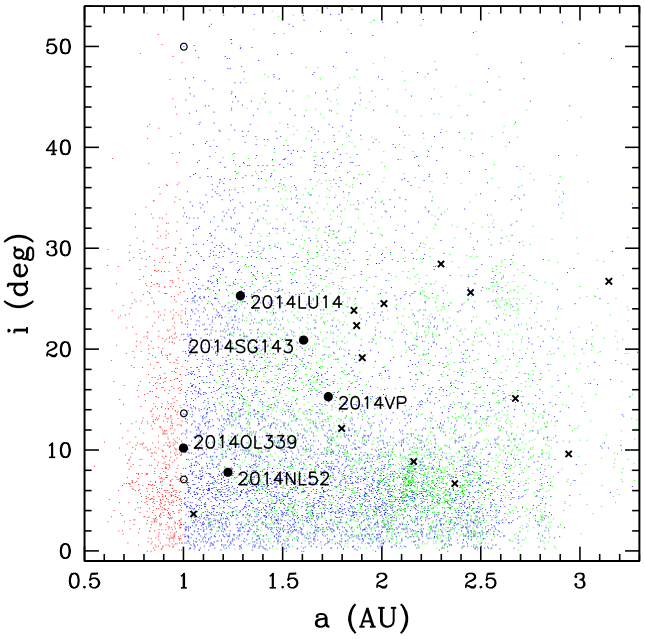

Figure 4. The classical *a*–*i* orbital distribution (inclination versus semimajor axis) including our discoveries (solid circles) and other NEA candidates (crosses) with respect to the entire known (green dots), Apollos (blue), and Atens populations (red dots). With open circles, we plot the other three known Earth quasi-satellites, in comparison with 2014 OL339. The Jupiter trojan 2014 RC13 is located outside the plot ($a = 5.2$ au).

3.1 2014 LU14, the first NEA discovered from La Palma

Designated as EUHT171 by the actual discoverer Lucian Hudin who analysed images with ASTROMETRICA, this NEA candidate was imaged first on 2014 June 2 at 04:17 UT in the field of the one-opposition NEA 2012 MR7 observed by the ING student V. Tudor during our C136 trigger of the regular INT programme C106 (PI: L. Verdes-Montenegro).

With an MPC NEO score Int=100 and situated close to the border of the ϵ–μ model (Vaduvescu et al. 2011a, which is less efficient at lower solar elongations), this NEA candidate was secured and followed on four nights with the INT by the observers O. Vaduvescu during the C106 run, A. Kong and R. Jin during the next C50 run (PI: D. Torres) and O. Vaduvescu and M. Popescu during the N8 run (PI: O. Vaduvescu). Finally, this Apollo object received permanent designation 2014 LU14 (MPS 518060 and 518856) and became the first EURONEAR NEA discovered and secured from La Palma and using the INT telescope (ING, 2014).

3.2 2014 NL52, a very fast rotator

The actual discoverer Lucian Hudin reported an unknown long trail in one of the fields of our main target PHA 2010 SH13 observed in the morning of 2014 July 10 at 04:36 UT during the Spanish CAT service night attended by O. Zamora. Designated EUHT288, this fast NEA candidate was moving with a proper motion of $\mu = 6.1$ arcsec s^{-1} at relatively low solar elongation $\epsilon = 93°$, resulting in an MPC NEO score 100 and being placed well above the NEO limit on the ϵ–μ model.

Due to the scheduled INT instrument change, next day we lost access to the telescope, so we alerted the EURONEAR nodes and other collaborators to secure this fast moving NEA. Fortunately, the Instituto de Astrofísica de Andalucía (IAA, one of the EURONEAR

nodes) responded promptly, and they used the 1.5 m telescope at OSN, based on DDT time granted at very short notice by S. Ruiz and R. Duffard, thus the observer A. Sota successfully recovered the object in one of the fields, securing our discovery.

Following the discovery night, our team gathered orbital and physical follow-up data on 12 nights, including the OSN 1.5 m telescope (observer A. Sota during five nights), the 2 m Liverpool Telescope (LT, proposal CQ14B01 during one night managed by J. Marchant also member of EURONEAR), the INT (during two D-nights observed by O. Vaduvescu, V. Tudor and T. Mocnik) and the Tautenburg 2 m TLS telescope at the Karl Schwarzschild Observatory (during four nights observed by B. Stecklum, another member of EURONEAR). This object was also observed spectroscopically with the 10.4m Gran Telescopio Canarias (GTC, PI: J. de Leon, observer: C. Alvarez, reducer: A. Cabrera-Lavers). We will discuss the physical data in Section 4. In the meantime, this Apollo object received designation 2014 NL52, becoming the second EURONEAR NEA discovery (MPS 522840, 523438, 524006, 531624, 533418).

3.3 2014 OL339, the fourth known Earth quasi-satellite

Designated as EURC061 by its actual discoverer Farid Char, this NEA candidate was observed at 2014 July 29 02:51 UT during an INT D-night attended by O. Vaduvescu and V. Tudor, in the main target field NEA 2013 VQ4. The detection of this unknown object was quite difficult (the most difficult from all our discoveries) due to its faintness ($R \sim 21.9$) and relatively fast proper motion ($\mu = 2.1$ arcsec s^{-1}) which resulted in small trails in the vicinity of two stars, probably escaping detection by an automated pipeline. Observed at relatively low solar elongation ($\epsilon = 117^\circ$), the object immediately became an NEA candidate with an MPC NEO score 100 and located well above the NEA limit on the ϵ–μ model.

During next night, we could secure our discovery using the INT, triggering some time during our own NEA photometry programme N8 (PI: O. Vaduvescu), then we could follow-up two more nights, thanks to our C136 ToO programme (during one D-night observed by T. Mocnik) and also during our new P2 ToO programme triggered during the regular UK P1 programme (PI: V. Dhillon joined by observer D. Sahman). While fitting the data using the FIND_ORB software (Gray 2015), O. Vaduvescu noticed an orbit very close to the Earth ($a \sim 0.999$ au). Finally, this Aten object was published as 2014 OL339 (MPS 525771) and became our third EURONEAR-discovered and secured NEA which indeed turned out to be a very rare NEA to be discussed in Section 5.

3.4 2014 SG143, our largest discovered NEA

Designated EUHT461, this brighter NEA candidate ($R = 20.5$) was discovered by Lucian Hudin in the field of the main target NEA 2011 XE1 observed in the morning of 2014September 18 at 03:51 UT, during a D-night attended by O. Vaduvescu, T. Mocnik and M. Popescu. Moving relatively slowly ($\mu = 1.0$ arcsec s^{-1}) but relatively far from opposition ($\epsilon = 145^\circ$), the object became an obvious NEA candidate with a score of 98 and being located above the ϵ–μ plot.

Thanks to our new 2014B UK P2 programme, the following night we were able to override the P10 programme (PI: B. T. Gänsicke, observer M. Hollands) to secure this NEA candidate. Then, the collaborators M. Micheli and D. Koschny scheduled some follow-up observations using the 1 m Optical Ground Station of the European Space Agency (ESA-OGS, observer M. Busch, reducers A. Knofel and E. Schwab) which confirmed its NEA status. Finally, this Amor object was officially named 2014 SG143 (MPS 533750) and became our fourth NEA discovered from La Palma and using the INT. This is actually a large object and our largest NEA discovery, estimated between 0.6 and 1.4 km (NEODyS and EARN data base) based on its absolute magnitude $H = 18.4$.

3.5 2014 VP, the brightest NEA discovery

Designated as EUHR001 by its actual discoverers Lucian Hudin and Radu Cornea, this NEA candidate was seen on 2014 November 4 05:20 UT during an INT D-night, being observed by the ING students T. Mocnik, M. Díaz Alfaro, I. Ordonez-Etxeberria and F. Lopez-Martinez in the field of the target NEA 2004 CL1. This relatively bright object ($R \sim 19.3$ and our brightest discovered NEA) was trailing due to its fast proper motion ($\mu = 5.3$ arcsec s^{-1}), the two ends of the trail being averaged and reported within hours to the MPC. Observed at $\epsilon = 143^\circ$ solar elongation, this object became an obvious NEA candidate with an MPC NEO score 100 and clearly located well above the NEA limit on the ϵ–μ model.

Despite the targeted recovery observation of the Spacewatch survey which recovered our NEA six hours later, the predicted positional uncertainty for the second night reached about 0.5, while the weather at ORM and Moon conditions remained very poor. Once again, the EURONEAR network was alerted to recover this object, and fortunately our Poznan EURONEAR node (observers T. Kwiatkowski and K. Kaminski) was able to recover the object using their 0.7 m PST2 remote telescope located at the Winer Observatory in Arizona. The following night, a battery of three telescopes (OSN 1.5 m with observer V. Casanova, IAC80 with observer M. Gomez-Jimenez and INT with observers T. Mocnik service observer of a run PI: I. Negueruela), followed by O. Vaduvescu and collaborators using the 1.2 m Mercator and B. Stecklum using the TLS 2 m telescopes enlarged the arc and firmed the orbit of this Apollo NEA which officially became 2014 VP and our fifth EURONEAR NEA discovered using the INT from La Palma.

3.6 EUHT400, a small object lost due to lack of follow-up time and very rapid motion

The reducer Lucian Hudin reported a very long trail caused by the unknown object designated EUHT400 at 2014 August 4 01:40 UT, in the corner of a frame taken by V. Dhillon (PI of P1 programme) and co-observer D. Sahman, triggered by our P2 NEA override programme. Moving very fast ($\mu = 11.2$ arcsec s^{-1}) and very close to opposition ($\epsilon = 176^\circ$), this was our most obvious NEA candidate with an MPC score 97 and located very high on the ϵ–μ model.

Although we immediately alerted our EURONEAR nodes and collaborators, unfortunately none was able to follow-up the object during the next night. Not being allowed to trigger additional time at the INT, we asked the INT observer R. Génova-Santos (ITP13-8 programme, PI: Rubino-Martin) who kindly accepted a very short window in the hope of recovering EUHT400 pointing the telescope to three neighbouring fields spanning across the very elongated sky uncertainty ellipse ($\sim 2^\circ$ major axis). Unfortunately, the object did not show up in any of these images, although at least one other fast moving object (denoted as EUVI016 which does not match the EUHT400 orbit) was found after very careful analysis a few months later by Victor Inceu. During the next night, the recovery of EUHT400 became impossible due to sky-rocketing uncertainty (estimated by MPC to at least 10°), so we lost this discovered NEA, unfortunately.

3.7 Other NEA candidates

Besides the above six obvious NEA discoveries, between 2014 Feb and Nov as part of our INT ToO programmes, our team followed up 14 unknown objects considered NEA candidates based on their MPC NEO Int score (choosing a lower 20 per cent threshold for safety) and also the ϵ–μ model (Vaduvescu et al. 2011a). We include these objects in Table 2, plotting them with crosses in Figs 2, 3 and 4, and we discuss next some of these objects.

Although located around the ϵ–μ NEA limit (plotted as a magenta dotted line in Fig. 2) and observed close to opposition, up to six NEA candidates turned out to be regular main belt asteroids, namely the objects EUHTT05 (designated as 2014 FY32, MPS 506887), EUMO086 (2014 OG361, MPS 525793), EUHT275 (MPC score 23 and moving perpendicular on the direction of other MBAs in the field), EUHT251 (score 25), EUMO207 (score 51) and EUMO208 (score 33, followed-up from Modra 0.6m and GLORIA D50 0.5m Ondrejov telescopes).

The very fast object EUHT308 ($\mu = 6.3$ arcsec min^{-1}) resulted in a long trail and became an obvious NEA candidate (score 100), being reported immediately to MPC. Nevertheless, this object was discovered by Pan-STARRS two days before, our INT recovery observations confirming its Amor orbit (MPS 524257).

Two NEA candidates, namely EUHT164 (designated as 2014 LP9, MPS 518055, 518856, $\mu = 1.4$ arcsec min^{-1} observed at very low solar elongation $\epsilon = 50^\circ$, MPC Int score 91) and EURC055 (score 27) have found to be Mars crossers.

Our faintest NEA candidate EURM074 ($R = 21.8$) was observed to move relatively fast ($\mu = 2.3$ arcsec min^{-1}) at relatively low solar elongation ($\epsilon = 87^\circ$), consistent with its MPC score 100. Unfortunately, the object could not be recovered during the second night (up to a deeper $r \sim 22.5$ limit), so these findings should be regarded with caution. Its very short arc (7 min) could be fit by FIND_ORB in a near circular Earth-like orbit of Arjuna class.

Two more objects, namely EUHT309 (designated 2014 OH198, MPS 526663, 528326, discovered by Pan-STARRS) and EUHT462 (designated 2014 SP62, MPS 533673, discovered by INT and followed-up by ESA-OGS 1m) were found to be Hungarias.

The object EUMO201 (designated as 2014 RC13, MPS 531887, discovered by INT) could be recovered in twilight with the WHT 4.2 m telescope (observer: F. C. Riddick) and OSN 1.5 m twice (observer: V. Casanova) but could not be seen few days later, using neither the C2PU 1 m, nor the LT 2 m. Its three-day arc orbit corresponds to a Jupiter trojan.

Finally, while scrutinizing recently the three recovery fields of the lost EUHT400, Victor Inceu discovered another fast moving object (denoted EUVI016, $\mu = 6.1$ arcsec min^{-1}, Int score 100), although this NEA does not match the previous night EUHT400 orbit.

4 THE VERY FAST ROTATOR 2014 NL52

Based on the INT discovery images showing our long trail object EUHT288 and also based on the OSN follow-up images, L. Hudin visually noticed rapid variation in brightness, suggesting first that the new object could be a fast rotator. To study rotation, O. Vaduvescu secured 2 h in the Liverpool 2 m telescope (LT) and later 2 h with the INT, part of his Dutch N8 programme for light curves of NEAs.

4.1 Rotation period

The asteroid was observed photometrically on 2014 July 20/21 with the 1.5 m telescope at the OSN observatory. Due to the object's faintness ($V \sim 20$ mag), the EEV 42-40 CCD mounted at the telescope was used without any filters. The exposure time was 60 s with a 2 s readout. The data were reduced using the LIDAS package (Lightcurve Derivation for Asteroids) written in PYTHON by the ING student Vlad Tudor. The light curve obtained from the 0.62 h run revealed a possible rotation period of $P_1 = 4.43 \pm 0.03$ min but its significance was questionable, due to high noise.

A confirmation of the asteroid short period was obtained on 2014 July 29/30 when 2014 NL52 was observed with the INT. The object was observed for 1.86 h using the SDSS r filter. The exposure time was 20 s, with a duty cycle of 25 s using a 5 arcmin × 5 arcmin window in CCD4. The data were reduced using the same LIDAS package. The light curve was analysed by iteratively fitting a Fourier series using different trial periods (Kwiatkowski et al. 2009). The best fit was obtained for two synodic periods: $P_2 = 4.459 \pm 0.003$ min and $P_3 = 8.917 \pm 0.004$ min which is quite common in case of noisy light curves. It is important to note that the light-curve peak-to-peak amplitude was $A \approx 0.6$ mag, and the solar phase angle was ($\alpha = 58^\circ$). To analyse such ambiguities, we used simulations of Butkiewicz et al. (2014) in which light curves were obtained for different model shapes, spin axes and illuminations. All light curves simulated at $\alpha = 58^\circ$ and $A = 0.6$ mag had two maxima and two minima per period. This let us believe the P_2 solution represents the true period of 2014 NL52 so that we assign it a reliability code $U = 2+$ (Warner, Harris & Pravec 2009). We did not attempt to fold the July 20 and 29 data because the 3σ uncertainty in the derived synodic period, after 9 d, would lead to the uncertainty in the rotation phase as large as six rotations.

The composite light curve obtained with $P_2 = 4.459 \pm 0.003$ is presented in Fig. 5. Its peak-to-peak amplitude of $A \approx 0.6$ mag can be used to estimate the asteroid minimum elongation $\frac{a}{b}$, where a and b are the semi-axes of the triaxial shape approximation. Using the relation from Kwiatkowski et al. (2010)

$$\frac{a}{b} \geq 10^{0.4A(\alpha)/(1+0.03\,\alpha)}, \quad (1)$$

where $A(\alpha)$ is a peak-to-peak amplitude, observed at a phase angle α, we obtain for 2014 NL52 $\frac{a}{b} \geq 1.2$.

4.2 Spectra and suggested composition

A low-resolution spectrum of 2014 NL52 was obtained on 2014 August 15 using the Optical System for Imaging and Low Resolution Integrated Spectroscopy (OSIRIS) camera-spectrograph (Cepa et al. 2000; Cepa 2010) at the 10.4m GTC located at the ORM observatory. The OSIRIS instrument consists of a mosaic of two Marconi CCD detectors, each with 2048 × 4096 pixels and a total unvignetted field of view of 7.8 arcmin × 7.8 arcmin, giving a plate scale of 0.127 arcsec pixel^{-1}. To increase the signal-to-noise ratio for our observations, the data were 2 × 2 binned, corresponding to the standard operation mode of the instrument. We used the R300R grism (dispersion of 3.87 Å pixel^{-1}) and a 5 arcsec slit, oriented at the parallactic angle to minimize slit losses due to atmospheric dispersion. We obtained three spectra with an exposure time of 600 s each.

Images were bias- and flat-field corrected, using lamp flats. The two-dimensional spectra were wavelength calibrated using Xe+Ne+HgAr lamps. After the wavelength calibration, the sky background was subtracted and a one-dimensional spectrum was

Table 2. The observing log and circumstances for the six NEAs discovered with the INT and the other 14 NEA candidates.

Obs[1]	Designation	Nickname	Disc. date UT	Target NEA	μ	ϵ	Score	EXP	Img	R	a	e	i	MOID	H	Orbit	FN	Arc
NEA discoveries:																		
(1)	2014 LU14	EUHT171	02 Jun 04:17	2012 MR7	0.9	111	100	120	6	21.6	1.2871	0.45	25.32	0.1973	19.6	Apollo	4	85 d
(2)	2014 NL52	EUHT288	10 Jul 04:36	2010 SH13	6.1	94	100	120	6	20.7	1.2239	0.19	7.76	0.0059	23.6	Apollo	12	75 d
(3)	2014 OL339	EURC061	29 Jul 02:51	2013 VQ4	2.1	121	100	120	4	21.9	0.9993	0.46	10.19	0.0182	22.9	Aten	3	49 d
(4)	2014 SG143	EUHT461	18 Sep 03:51	2011 XE1	1.0	156	98	120	8	20.5	1.6055	0.29	20.90	0.2499	18.5	Amor	2	58 d
(5)	2014 VP	EUHR001	04 Nov 05:20	2004 CL1	5.3	143	100	120	6	19.3	1.7301	0.42	15.35	0.0529	22.8	Apollo	4	17 d
(6)	– (lost)	EUHT400	04 Aug 01:40	EUMO086	11.2	182	100	120	6	22.2	∼1.4	∼0.4	∼3	∼0.001	∼30	NEA	–	20 m
NEA candidates:																		
(7)	2014 FY32	EUHTT05	23 Mar 00:56	2012 VF5	1.1	177	15	120	8	21.5	1.7977	0.29	12.15	0.3186	22.0	MBA	1	4 d
(8)	2014 LP9	EUHT164	01 Jun 03:49	2012 MR7	1.4	50	91	120	4	20.7	2.9430	0.49	9.62	0.4955	19.5	Mars crosser	3	34 d
(9)	–	EURC055	24 Jun 01:32	2010 RN82	0.8	165	27	150	8	20.6	2.0113	0.19	24.52	0.6543	18.0	Mars crosser	1	6 d
(10)	–	EUHT275	24 Jun 00:24	2010 JH88	0.9	199	23	150	7	19.9	2.4487	0.21	25.62	0.9319	18.2	MBA	1	6 d
(11)	–	EUHT251	24 Jun 01:07	2013 PY38	1.2	186	25	120	8	20.1	2.2992	0.17	28.45	0.8976	18.5	MBA	1	6 d
(12)	2014 OG361	EUMO086	29 Jul 00:37	2013 EW27	0.5	141	24	120	6	21.1	1.8731	0.07	22.34	0.7843	19.9	MBA	3	6d
(13)	–	EURM074	29 Jul 03:08	2013 MR	2.3	87	100	60	4	21.8	∼1.1	∼0.1	∼4	∼0.003	∼26	Arjuna?	–	7 m
(14)	2014 OQ207	EUHT308	29 Jul 03:50	2005 SX4	7.2	120	100	120	5	19.6	∼2.2	∼0.5	∼9	∼0.04	∼24	Amor	–	20 m
(15)	2014 OH198	EUHT309	29 Jul 03:50	2005 SX4	0.8	120	19	120	5	19.9	1.8592	0.06	23.85	0.7738	17.9	Hungaria	1	1 d
(16)	–	EUVI016	05 Aug 02:03	EUHT400-1	6.1	211	100	20	4	20.9	∼2.4	∼0.5	∼7	∼0.09	∼26	NEA	–	3 m
(17)	2014 RC13	EUMO201	02 Sep 05:12	2012 FO62	0.3	37	54	60	6	20.8	5.2143	0.04	24.74	0.8169	13.6	Jupiter trojan	3	4 d
(18)	–	EUMO207	17 Sep 20:40	2014 NL52	0.3	185	51	120	5	21.0	2.6741	0.41	15.12	0.6278	20.0	MBA?	–	19 m
(19)	–	EUMO208	17 Sep 20:40	2014 NL52	0.4	201	33	120	15	19.7	3.1458	0.28	26.73	1.2330	15.9	MBA?	3	1 d
(20)	2014 SP62	EUHT462	18 Sep 04:17	2011 ET4	0.9	150	36	120	10	20.1	1.9015	0.05	19.16	0.7978	18.6	Hungaria?	2	3 d

[1] Observers, reducers (with actual discoverer/s in bold), MPC publications, comments:
(1) O. Vaduvescu, V. Tudor, L. Hudin, M. Popescu (INT), MPS 518060, 518856, discovered by INT;
(2) O. Zamora, L. Hudin, V. Tudor, T. Mocnik, M. Popescu (INT) + A. Sota, L. Hudin (OSN 1.5 m) + B. Stecklum (TLS) + O. Vaduvescu, L. Hudin (LT) MPS 522840, 523438, 524006, 531624, 533418, disc. by INT;
(3) O. Vaduvescu, V. Tudor, F. Char, L. Hudin, T. Mocnik, V. Dhillon, D. Sahman (INT), MPS 525771, discovered by INT;
(4) O. Vaduvescu, T. Mocnik, M. Popescu, M. Hollands, L. Hudin (INT) + M. Busch, M. Micheli, D. Koschny, A. Knofel, E. Schwab (ESA-OGS), MPS 533750, discovered by INT;
(5) O. Vaduvescu, L. Hudin, R. Cornea, T. Mocnik, M. Díaz Alfaro, I. Ordonez-Etxeberria, F. López-Martinez, I. Negueruela (INT) + T. Kwiatkowski, K. Kaminski, L Hudin (PST2) + S. Gajdos (Modra) + M. Gomez-Jimenez, L. Hudin, O. Zamora (IAC80) + O. Vaduvescu, M. Popescu, F. Stevance and D. Morate (Mercator) + B. Stecklum (TLS), MPS 544906, 545885, MPEC W07, V71, discovered by INT;
(6) PI: V. Dhillon, D. Sahman, L. Hudin, V. Inceu, O. Vaduvescu, R. Génova-Santos (INT), estimated FIND_ORB orbit based on very short arc, discovered by INT (lost object);
(7) PI: S. Hidalgo, S. Murabito, L. Hudin, V. Tudor (INT), MPS 506887, discovered by INT;
(8) O. Vaduvescu, L. Hudin, V. Tudor, PI: L. Verdes-Montenegro (INT), MPS 518055, 518856, discovered by INT;
(9) O. Vaduvescu, V. Tudor, F. Char (INT), Mars MOID 0.0035;
(10) O. Vaduvescu, V. Tudor, L. Hudin (INT), moving perpendicular on other MBAs;
(11) O. Vaduvescu, V. Tudor, L. Hudin (INT);
(12) O. Vaduvescu, V. Tudor, T. Mocnik (INT), MPS 525793, discovered by INT;
(13) O. Vaduvescu, V. Tudor, S. Mihalea, L. Hudin (INT), not found next night;
(14) O. Vaduvescu, V. Tudor, L. Hudin (INT), MPS 524257, discovered by Pan-STARRS;
(15) O. Vaduvescu, V. Tudor, L. Hudin (INT), MPS 526663, 528326, discovered by Pan-STARRS;
(16) R. Génova-Santos, O. Vaduvescu, V. Inceu (INT), discovered few months late after careful scrutiny in the EUHT400 one follow-up field, estimated FIND_ORB orbit based on very short arc (lost object);
(17) O. Zamora, J. Font, A. Bereciartua, T. Mocnik, V. Tudor (INT) + F. Ridick, L. Hudin (WHT); V. Casanova, L. Hudin (OSN) + J. P. Rivet, L. Abe, P. Bendjoya, D. Vernet (C2PU), MPS 531887, discovered by INT;
(18) O. Vaduvescu, T. Mocnik, M. Popescu, R. Cornea (INT), not found later during three attempts;
(19) O. Vaduvescu, T. Mocnik, M. Popescu (INT) + S. Gajdos, P. Veres (Modra) + M. Serra-Ricart (GLORIA);
(20) O. Vaduvescu, T. Mocnik, M. Popescu (INT) + D. Abreu Rodriguez (OGS); L. Hudin, M. Popescu (INT) + M. Micheli, D. Koschny, M. Busch, A. Knofel, E. Schwab (OGS), MPS 533673, discovered by INT.

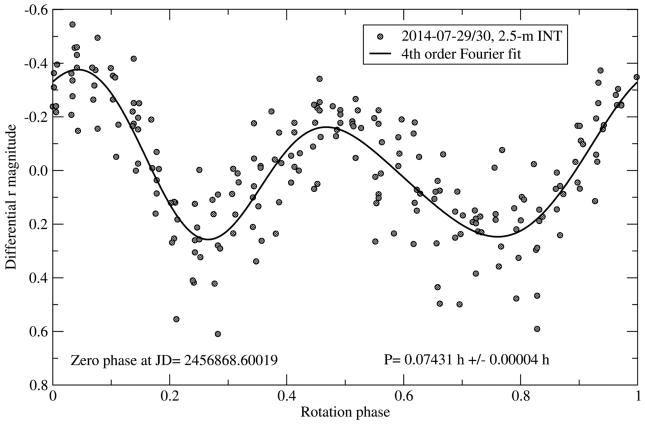

Figure 5. A composite light curve of 2014 NL52, observed on 2014 July 29/30 with the INT. It was obtained with the rotation period of $P_2 = 4.459$ min. A fourth-order Fourier series fit, used to derive the period, has been superimposed on the data.

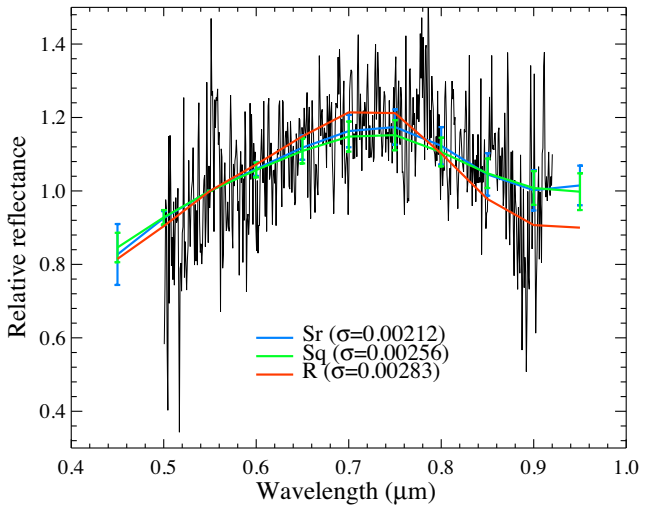

Figure 6. The visible spectrum of 2014 NL52 obtained with OSIRIS at GTC. The mean spectrum of Sr-, Sq- and R-type asteroids from DeMeo et al. (2009) are shown in blue, green and red, respectively. Values in parenthesis indicate the standard deviation of the χ^2 fit for each taxonomic type.

obtained. To correct for telluric absorption and to obtain the relative reflectance, the solar-analogue stars SA110-361 and SA112-1333 (Landolt 1992) were observed using the same spectral configuration at an airmass nearly identical to that of the object. Each individual spectrum of the object was then divided by the corresponding spectra of the solar analogues. The resulting spectra were finally averaged and normalized to unity at 0.55 μm. The resulting final reflectance spectrum is shown in Fig. 6. We used the M4AST online tool (Popescu, Birlan & Nedelcu 2012) to classify our visible spectrum of NL52, finding that the asteroid is an S-type object.

4.3 Phase curve and size

One service proposal was granted to O. Vaduvescu to use the 4.2 m WHT, but the bright Moon and the rapidly fading asteroid prevented accurate photometric observations of 2014 NL52, unfortunately.

To derive the asteroid phase curve, we first used the data reported by the NEODyS service. We selected only the observations done in either *R* or *V* filters. Using an average colour of the S-type NEAs of

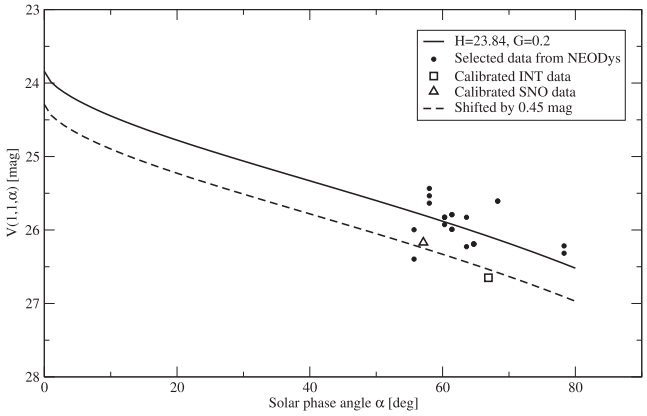

Figure 7. Phase curve of 2014 NL52. Black circles are approximative magnitudes, selected from the NEODyS server, transformed to the *V* band. Open triangles and squares are average asteroid magnitudes in *V* band, obtained from the light curves observed with the 1.5-m OSN telescope and 2.5-m INT. The *H*–*G* curve, fitted to the black circles, has been shifted downwards so that it goes close to the photometric measurements.

$V - R = 0.49$ mag (Shevchenko & Lupishko 1998), we transformed the *R*-band magnitudes to *V*, then we derived the *H* and *G* parameters of the phase curve by a least-square fit (Fig. 7). The obtained values are $H = 23.84$ mag, and $G = 0.2$. To check this result, we calculated the asteroid magnitudes (averaged over its rotation) from the July 20 OSN and July 29 INT data, calibrating them to the standard *V* magnitudes using the CMC15 and APASS stars found in the CCD images close to the asteroid. The OSN observations were made unfiltered, so to derive object's *V* magnitude we used two stars with the APASS SDSS $g - r$ colours of 0.91 and 0.32 mag. They were redder and bluer than the average colour of an S-type asteroid ($g - r = 0.62 \pm 0.02$, fig. 10 in Ivezic et al. 2001). The differential photometry of the asteroid using those two stars gave its average *r* magnitude of 20.91 and 21.01 mag, respectively, thus we accepted the mean of those two values: $r = 20.96$ mag. For the INT data obtained through the SDSS *r* filter, we determined the asteroid average *r* magnitude by comparing its brightness with two nearby stars, whose *r* magnitudes were reported by both CMC15 and APASS catalogues.

The asteroid *r* magnitudes were then converted to the *V* band using the standard equations given by Fukugita et al. (1996) with an average colour of S type ($g - r = 0.62$).

Adding together the two OSN and INT brightness measurements on the phase curve plot (Fig. 7), one can see that they are located well below the *H*–*G* fit. This is a common situation usually caused by the bias in magnitudes reported to the MPC with the astrometric measurements. Obviously, more accurate positions are derived from the CCD frames on which the asteroid is brighter, which favours light curve maxima. For this reason, we believe the phase curve should be shifted downwards by about 0.45 mag, so that it coincides with our photometric measurements, thus a new value for the absolute magnitude is $H = 24.29$ mag. We note that the $G = 0.2$ obtained from our fit is close to the average value of 0.24 derived for S-type asteroids (Warner et al. 2009). It is difficult to estimate the accuracy of the *H* value, so we assume the maximum systematic uncertainty of *H* to be 0.5 mag, thus the absolute magnitude for 2014 NL52 becomes $H = 24.3 \pm 0.5$ mag.

To derive the effective diameter of 2014 NL52, we use a standard procedure from Fowler & Chillemi (1992). Knowing that 2014 NL52 is an S-type object, we can assume its geometric albedo in *V* is

$p_V = 0.26^{+0.04}_{-0.03}$ (Thomas et al. 2011). Since we have only a systematic uncertainty for the H value, for the comparable uncertainty of the geometric albedo we adopt a 3σ value, so that $0.17 < p_V < 0.38$. With such values for H and p_V, we obtain the effective diameter $D = 36^{+20}_{-12}$ m where the uncertainties indicate an interval in which the true value can be found rather than standard deviations.

5 THE FOURTH DISCOVERED AND FIRST ATEN EARTH QUASI-SATELLITE 2014 OL339

A few weeks after our discovery of 2014 OL339, Carlos de la Fuente Marcos (Universidad Complutense de Madrid) contacted O. Vaduvescu to announce our team an interesting orbital discovery. According to their numerical models based on the currently known orbit, this object turned out to be the fourth ever known NEA to revolve in a quasi-satellite and quite unstable orbit with respect to the Earth, which started at least about 775 years ago and will end 165 years from now (de la Fuente Marcos & de la Fuente Marcos 2014).

Besides 2014 OL339, in Figs 3 and 4 we plot with open circles the other three known quasi-Earth satellites, namely the PHA (164207) 2004 GU9 discovered by LINEAR in 2004, the NEA (277810) 2006 FV35 discovered by Spacewatch in 2006, and the NEA 2013 LX28 discovered by Pan-STARRS in 2013, all three moving in Apollo orbits. In this context, EURONEAR discovered the fourth known Earth quasi-satellite 2014 OL339, which became actually the first such object moving in an Aten orbit, and besides (164207) being the most unstable of the known Earth quasi-satellites (de la Fuente Marcos & de la Fuente Marcos 2014).

Using larger field 2-m class surveys to discover fainter NEAs (such as 2014 OL339 at $R = 21.9$) is essential for increasing the known population of Earth quasi-satellites and characterizing the closest NEA sub-classes, such as PHAs or the newly defined Arjuna-type asteroids in Earth-like orbits (de la Fuente Marcos 2015). Moreover, the discovery of such fainter objects is important for identifying targets for future space missions, so in this sense 2-m class surveys (such as Pan-STARRS or Spacewatch) and even smaller NEA projects (such as EURONEAR using the INT-WFC) could bring major contributions to the NEA research.

6 UPDATED UNKNOWN NEA SKY DENSITY ACCESSIBLE TO 2-M SURVEYS

Based on our past INT-WFC data set collected by mid-2012 in a total 24 deg^2 survey, Vaduvescu et al. (2013a) estimated the unknown NEA sky density accessible to 2-m surveys, predicting in good conditions (clear and dark sky with seeing below $\sim$1.5 arcsec) a discovery rate of one NEA per two square degrees. We are checking now this statistics using our new 2014 data set.

Considering all the INT-WFC fields observed in the period 2014 Feb–Nov , we count a total of 158 fields observed in dark conditions, similar to those considered our previous work. Taking into account the WFC field of 0.28 deg^2, our 2014 data increase our actual total survey area to about 44 deg^2 (almost double compared with our past work). Considering our discovered NEAs, we can count between a minimum of eight NEAs (the five secured objects, the NEA EUHT308 discovered by Pan-STARRS, the lost EUHT400, plus the unknown rapid object EUVI016) and a maximum of 16 NEAs (considering the eight other NEA candidates located above or very close to the NEA limit on the ϵ–μ plot in Fig. 2). This gives an actual 2-m survey statistics of one NEA discovered in every 2.8 to 5.5 deg^2 (namely between 10 and 20 INT-WFC fields).

The above statistics should be regarded with caution due to our relatively small sky coverage, remaining to be probed by dedicated surveys. We are not aiming to address here the apparent NEA sky distribution based on our modest NEA recovery programme which could be affected by some selection and observational effects (Jedicke et al. 2002). Nevertheless, we can briefly compare now our 2014 statistics with the mid-2012 INT statistics (Vaduvescu et al. 2013a) which took into account all NEA candidates (none actually secured) which predicted one NEA discovery in every scanned 2 deg^2. During the past 2.5 years, about 2500 NEAs have been discovered mostly by 2-m class surveys (growing the number of known NEAs from $\sim$9000 to $\sim$11 500), actually dropping now our old discovery rate prediction to one NEA in every 2.7 deg^2. This expected NEA density matches very well our above discovery estimation rate (one NEA in each 2.8 deg^2) calculated after counting all 16 NEA candidates located above or very close to the NEA magenta limit dotted in the ϵ–μ plot in Fig. 2.

7 LESSONS LEARNED AND WORK IN PROGRESS

Three essential factors enabled us to discover and secure NEAs, namely:

(i) our INT override programmes which allowed short rapid access during available WFC nights;
(ii) the prompt data reduction in a team of students and amateurs available to reduce all fields and report NEA candidates within a few hours; and
(iii) the EURONEAR network able to contribute by accessing on short notice other telescopes in order to secure some discoveries.

Nevertheless, one very rapid NEA (EUHT400) escaped recovery during the next night and it was subsequently lost due to major sky growing uncertainty and lack of time on other 2-m class or larger telescope. To prevent such losses in the future, we implemented two measures:

(i) one data reduction staff will be available for first quick-look inspection of all images checking for longer trails (resulting in largest uncertainties following nights);
(ii) to save very fast objects including PHAs and Virtual Impactors (VIs), it is essential to secure some follow-up time using other facilities, so we secured LCOGT, IAC80, ESA-OGS and would ideally need the CFHT-MegaCam (best option in the north).

Our main NEA orbital improvement programme continues in 2014B and 2015A based on multiple TAC allocation time, with the aim of recovering with the INT more than half the entire known one-opposition NEA population in 2015, and serendipitously discovering a few more NEAs.

ACKNOWLEDGEMENTS

The PI thanks to the Spanish and UK TACs for allocations of override programmes C136/2014A, C88/2014B and P2/2014B based on which these first NEA EURONEAR, INT and La Palma discoveries took place. KK acknowledges support from the Polish Narodowe Centrum Nauki Grant UMO-2011/01/D/ST9/00427. LVM has been also supported by Grant AYA2011-30491-C02-01, co-financed by MICINN and FEDER funds, and the Junta de Andalucia (Spain) Grant TIC-114. SG was supported by the Slovak Grant Agency for Science VEGA, grant no. 1/0225/14. The research

leading to these results has received funding from the European Research Council under the European Union's Seventh Framework Programme (FP/2007-2013)/ERC Grant Agreement no. 320964 (WDTracer). The paper is based on override time and some D-time observations made with the INT operated on the island of La Palma by the ING in the Spanish ORM of the IAC. The following 11 telescopes participated in follow-up observations: the 1.5 m in OSN, Tautenburg 2 m TLS in Germany, the 2 m LT, Mercator 1.2 m telescopes and the 4.2 m WHT in La Palma, C2PU 1 m in France, Modra 0.6 m in Slovakia, Poznan 0.7 m (PST2) in Arizona, GLORIA D50 0.5 m in Ondrejov (remotely controlled), the 1 m ESA-OGS and IAC80 telescopes operated on the island of Tenerife by the IAC in the Spanish Observatorio del Teide. For image reduction, we used THELI (Erben et al. 2005; Schirmer 2013) and IRAF, a software package distributed by the National Optical Astronomy Observatory, which is operated by the Association of Universities for Research in Astronomy under cooperative agreement with the National Science Foundation. This research has made use of SAOIMAGE DS9, developed by Smithsonian Astrophysical Observatory. This research was made possible through the use of the AAVSO Photometric All-Sky Survey (APASS), funded by the Robert Martin Ayers Sciences Fund. Based on data from CMC15 Data Access Service at CAB (INTA-CSIC). Acknowledgments are due to Bill Gray for providing, developing and allowing free usage of FIND_ORB to the entire amateur-professional community. This research has made intensive use of the ASTROMETRICA software developed by Herbert Raab, a program very simple to install and use by students and amateur astronomers. We thank the MPC, especially T. Spahr and G. Williams who promptly revised some of our MPC reports. Acknowledges are also due to the anonymous referee for rapid response and suggestions to improve our paper.

REFERENCES

Birlan M., Vaduvescu O., Nedelcu D. A., Euronear Team, 2010a, Rom. Astron. J., 20, 119
Birlan M. et al., 2010b, A&A, 511, 40
Butkiewicz E. et al., 2014, in Muinonen K. et al., eds, Asteroids, Comets, Meteors 2014: Statistical Analysis of the Ambiguities in the Asteroid Period Determinations, Helsinki, Finland
Cepa J. et al., 2000, in Masanori I., Moorwood A. F., eds, Proc. SPIE Conf. Ser. Vol. 4008, Optical and IR Telescope Instrumentation and Detectors. SPIE, Bellingham, p. 623
Cepa J., 2010, in Diego J. M., Goicoechea L. J., González-Serrano J. I., Gorjas J., eds, Highlights of Spanish Astrophysics V. Springer-Verlag, Berlin, p. 15
de la Fuente Marcos C., de la Fuente Marcos R., 2014, MNRAS, 445, 2985
de la Fuente Marcos C., de la Fuente Marcos R., 2015, Astron. Nachr., 336, 5
DeMeo F. E., Binzel R. P., Slivan S. M., Bus S. J., 2009, Icarus, 202, 160
Erben T. et al., 2005, Astron. Nachr., 326, 432
Fowler J. W., Chillemi J. R., 1992, in Tedesco E. R. et al., eds, The IRAS Minor Planet Survey: IRAS Asteroid Data Processing. Phillips Laboratory, Kirtland AFB, NM
Fukugita M., Ichikawa T., Gunn J. E., Doi M., Shimasaku K., Schneider D. P., 1996, AJ, 111, 1748
Gray B., 2015, Find_Orb Orbit Determination Software. Available at: http://www.projectpluto.com/find_orb.htm
Isaac Newton Group 2014, Discovery of Near Earth Asteroid 2014 LU14 with the Isaac Newton Telescope, ING News. Available at: http://www.ing.iac.es/PR/press/1stnea.html
Ivezic Z. et al., 2001, AJ, 122, 2749
Jedicke R. et al., 2007, BAAS, 39, 421
Jedicke R., Larsen J., Spahr T., 2002, in Bottke W., ed., Asteroids III, Observational Selection Effects in Asteroid Surveys and Estimates of Asteroid Population Sizes. Univ. Arizona Press, Tucson, AZ, p. 71
Jet Propulsion Laboratory 2015, NEO Groups Page. Available at: http://neo.jpl.nasa.gov/neo/groups.html
Kwiatkowski T. et al., 2009, A&A, 495, 967
Kwiatkowski T. et al., 2010, A&A, 509, 94
Landolt A. U., 1992, AJ, 104, 340
Mainzer A. et al., 2011, AJ, 731, 53
Mainzer A. et al., 2012, ApJ, 752, 110
Minor Planet Center 2015, Available at: http://www.minorplanetcenter.net
Morbidelli A. et al., 2002, in Bottke W. F., Jr Cellino A., Paolicchi P., Binzel R. P., eds, Asteroids III, Origin and Evolution of Near-Earth Objects. Univ. Arizona Press, Tucson, AZ, p. 409
Popescu M., Birlan M., Nedelcu D. A., 2012, A&A, 544, 130
Raab H., 2015, Astrometrica. Available at: http://www.astrometrica.at
Schirmer M., 2013, ApJS, 209, 21
Shevchenko V. G., Lupishko D. F., 1998, Sol. Syst. Res., 32, 220
Skvarc J., 2015, FITSBLINK Calculation of Residuals of Asteroid Positions. Available at: http://www.fitsblink.net/residuals
Thomas C. A. et al., 2011, AJ, 142, 85
Vaduvescu O. et al., 2008–2014, About 100 MPC and MPEC Publications, Minor Planet Center, Harvard-Smithsonian Center for Astrophysics, Cambridge, MA, USA
Vaduvescu O., Birlan M., Colas F., Sonka A., Nedelcu A., 2008, Planet. Space Sci., 56, 1913
Vaduvescu O., Curelaru L., Birlan M., Bocsa G., Serbanescu L., Tudorica A., Berthier J., 2009, Astron. Nachr., 330, 698
Vaduvescu O. et al., 2011a, Planet. Space Sci., 59, 1632
Vaduvescu O., Tudorica A., Birlan M., Toma R., Badea M., Dumitru D., Opriseanu C., Vidican D., 2011b, Astron. Nachr., 332, 580
Vaduvescu O. et al., 2013a, Planet. Space Sci., 85, 299
Vaduvescu O. et al., 2013b, Astron. Nachr., 334, 718
Vaduvescu O. et al., 2014, in Muinonen K. et al., eds, Asteroids, Comets, Meteors 2014: Around 1500 Near Earth Asteroid Orbits Improved Via EURONEAR, Helsinki, Finland
Warner B. D., Harris A. W., Pravec P., 2009, Icarus, 202, 134
Wright E. et al., 2010, AJ, 140, 1868

[1]*Isaac Newton Group of Telescopes, Apto. 321, E-38700 Santa Cruz de la Palma, Canary Islands, Spain*
[2]*Instituto de Astrofísica de Canarias (IAC), vía Láctea s/n, E-38200 La Laguna, Tenerife, Spain*
[3]*Institut de Mécanique Céleste et de Calcul des Éphémérides (IMCCE) CNRS-UMR8028, Observatoire de Paris, F-75014 Paris Cedex, France*
[4]*ROASTERR-1 Observatory, ROASTERR-1 Observatory, Cluj Napoca, 400645, Romania*
[5]*Unidad de Astronomia, Universidad de Antofagasta, Avda. Angamos 601, 1270300 Antofagasta, Chile*
[6]*Astronomical Observatory Institute, Faculty of Physics, A. Mickiewicz University, Sloneczna 36, PL-60-286 Poznań, Poland*
[7]*Departamento de Astrofísica, Universidad de La Laguna, E-38206 La Laguna, Tenerife, Spain*
[8]*Astronomical Institute of the Romanian Academy, 5 Cutitul de Argint, 040557 Bucharest, Romania*
[9]*Romanian Astronomical Society for Meteors and Astronomy (SARM), 130029 Targoviste, Romania*
[10]*Departamento de Física Aplicada I, E.T.S. Ingeniería, Universidad del País Vasco, Alameda Urquijo s/n, E-48013 Bilbao, Spain*
[11]*Thuringer Landessternwarte Tautenburg, Sternwarte 5, D-07778 Tautenburg, Germany*
[12]*Instituto de Astrofísica de Andalucía (IAA-CSIC), Glorieta de la Astronomía, s/n, E-18008 Granada, Spain*
[13]*ESA NEO Coordination Centre, I-00044 Frascati (RM), Italy*
[14]*SpaceDyS s.r.l., I-56023 Cascina (PI), Italy*
[15]*INAF-IAPS, I-00133 Rome (RM), Italy*
[16]*Research and Scientific Support Department, European Space Agency, NL-2201 Noordwijk, the Netherlands*

[17] *Starkenburg-Sternwarte e.V. D-64646 Heppenheim, Germany*
[18] *Lindenberg Meteorological Observatory, D-16321 Lindenberg, Germany*
[19] *Taunus Observatory of the Physikalischer Verein, D-60486 Frankfurt, Germany*
[20] *Departamento de Física, Ingeniería de Sistemas y Teoría de la Señal, Escuela Politécnica Superior, University of Alicante, E-03690 Alicante, Spain*
[21] *Department of Physics and Astronomy, University of Sheffield, Sheffield S3 7RH, UK*
[22] *Astrophysics Research Institute, Liverpool John Moores University, IC2, Liverpool Science Park, 146 Brownlow Hill, Liverpool L3 5RF, UK*
[23] *Department of Physics, University of Warwick, Coventry CV4 7AL, UK*
[24] *Institute of Astronomy and Department of Physics, National Tsing Hua University, Hsinchu 30013, Taiwan*
[25] *Department Lagrange, Université de Nice Sophia-Antipolis, CNRS, Observatoire de la Cote d'Azur, CS34229, F-06304 Nice Cedex 4, France*
[26] *Observatoire de la Cote d'Azur, CS34229, F-06304 Nice Cedex 4, France*
[27] *Department of Astronomy, Physics of the Earth, and Meteorology, FMPI, Comenius Univ., Bratislava 842 48, Slovakia*
[28] *Ataman Science S.L.U., E-38290 Tenerife, Spain*

This paper has been typeset from a TEX/LATEX file prepared by the author.